IOPscience iopscience.iop.org

Home Search Collections Journals About Contact us My IOPscience

Coupled ferro–antiferromagnetic Heisenberg bilayers investigated by many-body Green function theory

This article has been downloaded from IOPscience. Please scroll down to see the full text article.

2005 J. Phys.: Condens. Matter 17 5059

(http://iopscience.iop.org/0953-8984/17/33/010)

View the table of contents for this issue, or go to the journal homepage for more

Download details:
IP Address: 129.252.86.83
The article was downloaded on 28/05/2010 at 05:50

Please note that terms and conditions apply.

INSTITUTE OF PHYSICS PUBLISHING JOURNAL OF PHYSICS: CONDENSED MATTER

J. Phys.: Condens. Matter **17** (2005) 5059–5072 doi:10.1088/0953-8984/17/33/010

Coupled ferro–antiferromagnetic Heisenberg bilayers investigated by many-body Green function theory

P Fröbrich[1,2,3], **P J Kuntz**[1] **and P J Jensen**[2]

[1] Hahn-Meitner-Institut Berlin, Glienicker Straße 100, D-14109 Berlin, Germany
[2] Institut für Theoretische Physik, Freie Universität Berlin, Arnimallee 14, D-14195 Berlin, Germany

E-mail: froebrich@hmi.de

Received 24 March 2005, in final form 30 June 2005
Published 5 August 2005
Online at stacks.iop.org/JPhysCM/17/5059

Abstract

A theory of coupled ferro- and antiferromagnetic Heisenberg layers is developed within the framework of a many-body Green function theory (GFT) that allows non-collinear magnetic arrangements by introducing sublattice structures. As an example, the coupled ferro–antiferromagnetic (FM–AFM) bilayer is investigated. We compare the results with those of bilayers with purely ferromagnetic or antiferromagnetic couplings. In each case we also show the corresponding results of mean field theory (MFT), in which magnon excitations are completely neglected. There are significant differences between GFT and MFT. A remarkable finding is that for the coupled FM–AFM bilayer the critical temperature decreases with increasing interlayer coupling strength for a simple cubic lattice, whereas the opposite is true for an fcc lattice as well as for MFT for both lattice types.

1. Introduction

In the interface region of coupled ferro- and antiferromagnetic systems there is a magnetic reordering known as the magnetic proximity effect (MPE). MPE has for a long time attracted the interest of researchers [1] since the constituents show a novel magnetic arrangement different from that of the bulk. The interest in such interfaces has revived lately with respect to the exchange bias effect [2], which occurs when a thin ferromagnetic (FM) film is deposited on an antiferromagnetic (AFM) material. If the latter is an 'in-plane AFM', and the number of bonds between parallel and antiparallel spin pairs across the interface is the same, the interface is 'compensated'. In this case the AFM often assumes an almost orthogonal magnetization with respect to the FM magnetic direction, while the spins of the AFM interface layer reside in a 'spin-flop-phase', in analogy to an AFM system in an external magnetic field [3].

[3] Author to whom any correspondence should be addressed.

 © 2005 IOP Publishing Ltd Printed in the UK

In previous studies investigating FM–AFM interfaces the magnetization of each FM layer is usually considered to be collinearly ordered and to rotate as a whole [4, 5]. Results concerning the spin reorientation transition (SRT) have been obtained for various magnetic systems but, to the best of our knowledge, only in the presence of magnetic anisotropies [5]. It is important to stress that, although we consider in the present work anisotropic interactions too, a non-collinear magnetization in coupled FM–AFM bilayers is caused mainly by isotropic exchange interactions. Whereas previous work describes a net magnetic reorientation of the total system, we consider the reorientation to take place in magnetic sublattices, leaving the net magnetic orientation of each layer almost unchanged. In the case of a compensated FM–AFM interface, the MPE extends to the FM layers close to the interface. Then, the magnetic structure of each FM layer is represented, in perfect analogy to the AFM layers, by two juxtaposed sublattices with different but uniform magnetization directions. Allowing a non-uniform intralayer magnetic structure in the FM subsystem leads to new features, which in turn are strongly dependent on the underlying lattice symmetry.

Often for simplicity, a mean field theory (MFT) is used to describe the magnetic reorientation. In a recent MFT [6] study of a coupled FM–AFM system for both sc(001) and fcc(001) lattices, a variety of different magnetic configurations emerge, depending on the parameter values. Usually the subsystem with the larger ordering temperature induces a magnetic order in the other one (MPE). For coupled sc(001) systems, both FM and AFM films are perturbed from their collinear magnetic order and exhibit similar behaviour. This symmetry is absent for fcc(001) films, which, under certain circumstances, may exhibit two different critical temperatures. An advantage of MFT is that many results can be derived analytically for simple bilayer systems.

We stress that, for thin magnetic films, collective magnetic excitations (spin waves) are particularly important. These are neglected completely by MFT. Such excitations are taken into account, for example, by many-body Green function theory. There is a large amount of work applying this theory to thin ferromagnetic films, in particular in connection with the reorientation of the magnetization as a function of temperature and film thickness. We mention only a few papers that cite further literature [7–10]. Antiferromagnetic films have also been treated, for example in [11, 12]. Not as much work has been done in which Green function theory treats the coupling of ferromagnetic layers to antiferromagnetic layers: in [13], a bilayer is investigated and [14] treats an extension to multilayers. In both cases, only a collinear magnetization is considered. In [15], a ferromagnetic film is coupled to an antiferromagnetic layer; however, the orientation of the magnetization of the antiferromagnet is frozen. Other work considers an antiferromagnetic coupling between ferromagnetic layers [16–18].

The new feature of the present work is to allow an in-plane reorientation of the magnetizations of the ferro- and antiferromagnetic layers due to the interlayer coupling as in the MFT approach of [6] but using Green function theory. We restrict ourselves to Heisenberg systems with spin $S = 1/2$ with an exchange anisotropy. We do not consider this an essential restriction, because we have shown in [19, 20] for ferromagnetic layers that through an appropriate choice of anisotropy parameters the exchange- and single-ion anisotropies yield very similar results, and that an appropriate scaling leads to universal magnetization curves for different spin quantum numbers. In the present paper, we examine in detail the magnetic arrangement of the simplest system: a perfectly ordered bilayer consisting of an FM monolayer that is coupled to an AFM monolayer. Thus, we do not address the exchange bias effect directly, since this effect is most likely related to a certain amount of interface disorder [21].

The paper is organized as follows. In section 2 we develop the Green function theory and discuss the method of solution for the resulting equations. In section 3 we present numerical results for bilayers with purely ferromagnetic or antiferromagnetic coupling as well as for

the coupled FM–AFM bilayer. In particular the effect of the interface coupling $J_{\rm int}$ on the characteristics and magnitude of the MPE at zero and finite temperatures is investigated. The resulting magnetic arrangements for various kinds of bilayer systems and for their corresponding ordering temperatures are determined. In section 4 we summarize the essential results and end with some remarks concerning further development.

2. The Green function formalism for coupling ferro- and antiferromagnetic layers

The starting point is an XXZ-Heisenberg Hamiltonian consisting of an isotropic Heisenberg exchange interaction with strength J_{ij} between nearest-neighbour lattice sites, exchange (non-localized) anisotropies in the x- or z-directions having strengths D^x_{ij} and D^z_{ij}, respectively, and an external magnetic field $\mathbf{B} = (B^x, 0, B^z)$ confined to the film plane, which is the xz-plane:

$$\mathcal{H} = -\tfrac{1}{2}\sum_{\langle ij\rangle} J_{ij}(S^-_i S^+_j + S^z_i S^z_j) - \tfrac{1}{2}\sum_{\langle ij\rangle}(D^x_{ij} S^x_i S^x_j + D^z_{ij} S^z_i S^z_j) - \sum_k (B^x S^x_i + B^z S^z_k). \tag{1}$$

Here the notation $S^{\pm}_i = S^x_i \pm \mathrm{i}S^y_i$ is introduced, and $\langle ij\rangle$ indicates summation over nearest neighbours only, where i and j are lattice site indices. Because there is no field B^y perpendicular to the film plane, only a reorientation of the magnetization in the xz-plane is allowed. For the FM–AFM bilayer we use D^z_{ij} in the ferromagnetic layer and D^x_{ij} in the antiferromagnetic layer.

In this paper we restrict ourselves to systems with spin quantum number $S = 1/2$ and to a simple cubic (sc) lattice. For this case we need the commutator Green functions

$$G^{\alpha-}_{ij}(\omega) = \langle\langle S^\alpha_i; S^-_j\rangle\rangle_\omega, \tag{2}$$

where $\alpha = (+, -, z)$ takes care of all directions in space. A generalization to spin quantum numbers $S > 1/2$ is straightforward by introducing $G^{\alpha,mn}_{ij} = \langle\langle S^\alpha_i; (S^z_j)^m (S^-_j)^n\rangle\rangle$ with $m + n \leqslant 2S + 1 (m \geqslant 0; n \geqslant 1; m, n$ integer) [7].

The equations of motion for the Green functions in the energy representation are

$$\omega G^{\alpha-}_{ij}(\omega) = A^{\alpha-}_{ij} + \langle\langle [S^\alpha_i, \mathcal{H}]; S^-_j\rangle\rangle_\omega \tag{3}$$

with the inhomogeneities

$$A^{\alpha-}_{ij} = \langle [S^\alpha_i, S^-_j]\rangle = \begin{pmatrix} 2\langle S^z_i\rangle\delta_{ij} \\ 0 \\ -\langle S^x_i\rangle\delta_{ij} \end{pmatrix}, \tag{4}$$

where $\langle\cdots\rangle = \mathrm{Tr}(\cdots \mathrm{e}^{-\beta\mathcal{H}})/\mathrm{Tr}(\mathrm{e}^{-\beta\mathcal{H}})$ denotes the thermodynamic expectation value.

In order to obtain a closed system of equations, the higher-order Green functions on the right-hand sides are decoupled by a generalized Tyablikov-(RPA) decoupling [7]

$$\langle\langle S^\alpha_i S^\beta_k; S^-_j\rangle\rangle_\eta \simeq \langle S^\alpha_i\rangle G^{\beta-}_{kj} + \langle S^\beta_k\rangle G^{\alpha-}_{ij}. \tag{5}$$

After introducing two sublattices per layer, which is necessary when dealing with antiferromagnets, the resulting equations are Fourier transformed to momentum space by

$$\begin{aligned} G^{\alpha-}_{mn}(\mathbf{k}) &= \frac{2}{N}\sum_{i_m j_n} G^{\alpha-}_{i_m j_n} \mathrm{e}^{-\mathrm{i}\mathbf{k}(\mathbf{R}_{i_m} - \mathbf{R}_{j_n})}, \\ G^{\alpha-}_{i_m j_n} &= \frac{2}{N}\sum_{\mathbf{k}} G^{\alpha-}_{mn}(\mathbf{k}) \mathrm{e}^{\mathrm{i}\mathbf{k}(\mathbf{R}_{i_m} - \mathbf{R}_{j_n})}, \end{aligned} \tag{6}$$

where i_m, j_n are lattice site indices on the sublattices m, n, and N is the number of lattice sites in the whole system. One obtains

$$\begin{aligned}
\omega G^{\pm-}_{mn} = {} & \begin{pmatrix} 2\langle S^z_m\rangle\delta_{mn} \\ 0 \end{pmatrix} \pm \left(B^z + \sum_p \langle S^z_p\rangle (J_{mp}(\mathbf{0}) + D^z_{mp}(\mathbf{0})) \right) G^{\pm-}_{mn} \\
& \mp \langle S^z_m\rangle \sum_p (J_{mp}(\mathbf{k}) + \tfrac{1}{2} D^x_{mp}(\mathbf{k})) G^{\pm-}_{pn} \mp \tfrac{1}{2}\langle S^z_m\rangle \sum_p D^x_{mp}(\mathbf{k}) G^{\mp-}_{pn} \\
& \mp \left(B^x + \sum_p \langle S^x_p\rangle (J_{mp}(\mathbf{0}) + D^x_{mp}(\mathbf{0})) \right) G^{z-}_{mn} \\
& \pm \langle S^x_m\rangle \sum_p (J_{mp}(\mathbf{k}) + D^z_{mp}(\mathbf{k})) G^{z-}_{pn}, \\
\omega G^{z-}_{mn} = {} & -\langle S^x_m\rangle\delta_{mn} - \tfrac{1}{2}\left(B^x + \sum_p \langle S^x_p\rangle (J_{mp}(\mathbf{0}) + D^x_{mp}(\mathbf{0})) \right) G^{+-}_{mn} \\
& + \tfrac{1}{2}\langle S^x_m\rangle \sum_p J_{mp}(\mathbf{k}) G^{+-}_{pn} + \tfrac{1}{2}\left(B^x + \sum_p \langle S^x_p\rangle (J_{mp}(\mathbf{0}) + D^z_{mp}(\mathbf{0})) \right) G^{--}_{mn} \\
& - \tfrac{1}{2}\langle S^x_m\rangle \sum_p J_{mp}(\mathbf{k}) G^{--}_{pn}.
\end{aligned} \tag{7}$$

For a square lattice with lattice constant $a_0 = 1$, one has four nearest-neighbour *intralayer* couplings with sublattice indices n, m from the same layer

$$\begin{aligned}
J_{mn}(\mathbf{0}) &= q_0 J_{mn}, & J_{mn}(\mathbf{k}) &= \gamma_0(\mathbf{k}) J_{mn}, \\
D^{x,z}_{mn}(\mathbf{0}) &= q_0 D^{x,z}_{mn}, & D^{x,z}_{mn}(\mathbf{k}) &= \gamma_0(\mathbf{k}) D^{x,z}_{mn},
\end{aligned} \tag{8}$$

with the *intralayer* coordination number $q_0 = 4$ and the momentum-dependent Fourier factor

$$\gamma_0(\mathbf{k}) = 2(\cos k_x + \cos k_z). \tag{9}$$

Correspondingly, for the nearest-neighbour *interlayer* couplings, with m, n now being sublattice indices from different layers, one obtains

$$\begin{aligned}
J_{mn}(\mathbf{0}) &= q_{\mathrm{int}} J_{\mathrm{int}}, & J_{mn}(\mathbf{k}) &= \gamma_{\mathrm{int}}(\mathbf{k}) J_{\mathrm{int}}, \\
D^{x,z}_{m,n}(\mathbf{0}) &= q_{\mathrm{int}} D^{x,z}_{\mathrm{int}}, & D^{x,z}_{mn}(\mathbf{k}) &= \gamma_{\mathrm{int}}(\mathbf{k}) D^{x,z}_{\mathrm{int}}.
\end{aligned} \tag{10}$$

For sc stacking, the *interlayer* coordination number and the corresponding Fourier factor are given by

$$q_{\mathrm{int}} = \gamma_{\mathrm{int}}(\mathbf{k}) = 1, \tag{11}$$

which is assumed in the following calculations if not stated otherwise.

For fcc or bcc stacking one has for comparison

$$q_{\mathrm{int}} = 4 \qquad \text{and} \qquad \gamma_{\mathrm{int}}(\mathbf{k}) = 4\cos(k_x/2)\cos(k_z/2). \tag{12}$$

The mean field approximation is obtained by neglecting the Fourier factors, i.e. $\gamma_0(\mathbf{k}) = \gamma_{\mathrm{int}}(\mathbf{k}) = 0$. By choosing the appropriate signs of the exchange interaction and the exchange anisotropy coupling constants, one can treat ferromagnetic, antiferromagnetic, and mixed systems with coupled FM and AFM layers.

The general formalism is valid for any number of layers and sublattices. If Z is the total number of sublattices of the system, the dimension of the set of equations (7) is $3Z^2$. Because we restrict ourselves in the present paper to the investigation of the bilayer problem, there are four sublattices, and the system of equations (7) is of dimension 48 with a corresponding

Green function vector. Closer inspection reveals that the system of equations has the following substructure:

$$\left(\omega\mathbf{1} - \begin{pmatrix} \mathbf{\Gamma} & 0 & 0 & 0 \\ 0 & \mathbf{\Gamma} & 0 & 0 \\ 0 & 0 & \mathbf{\Gamma} & 0 \\ 0 & 0 & 0 & \mathbf{\Gamma} \end{pmatrix}\right) \begin{pmatrix} \mathbf{G}_1 \\ \mathbf{G}_2 \\ \mathbf{G}_3 \\ \mathbf{G}_4 \end{pmatrix} = \begin{pmatrix} \mathbf{A}_1 \\ \mathbf{A}_2 \\ \mathbf{A}_3 \\ \mathbf{A}_4 \end{pmatrix}, \tag{13}$$

where the diagonal blocks $\mathbf{\Gamma}$ are identical 12×12 matrices, whose explicit form can be read off from equations (7). The sublattice Green functions $\mathbf{G}_n$ $(n = 1, 2, 3, 4)$ are vectors of dimension 12 consisting of four subvectors, each of dimension 3:

$$\mathbf{G}_n = \begin{pmatrix} \mathbf{G}_{1n} \\ \mathbf{G}_{2n} \\ \mathbf{G}_{3n} \\ \mathbf{G}_{4n} \end{pmatrix}, \qquad n = 1, 2, 3, 4, \tag{14}$$

where the 3-component vectors are

$$\mathbf{G}_{mn} = \begin{pmatrix} \mathbf{G}^{+-}_{mn} \\ \mathbf{G}^{--}_{mn} \\ \mathbf{G}^{z-}_{mn} \end{pmatrix}, \qquad m = 1, 2, 3, 4. \tag{15}$$

The inhomogeneity vectors have the same structure:

$$\mathbf{A}_n = \begin{pmatrix} \mathbf{A}_{1n}\delta_{1n} \\ \mathbf{A}_{2n}\delta_{2n} \\ \mathbf{A}_{3n}\delta_{3n} \\ \mathbf{A}_{4n}\delta_{4n} \end{pmatrix}, \qquad \mathbf{A}_{nm} = \begin{pmatrix} 2\langle S^z_m \rangle \\ 0 \\ -\langle S^x_m \rangle \end{pmatrix}, \qquad m, n = 1, 2, 3, 4. \tag{16}$$

The big equation (13) of dimension 48 for the bilayer can therefore be replaced by four smaller equations of dimension 12:

$$(\omega\mathbf{1} - \mathbf{\Gamma})\mathbf{G}_n = \mathbf{A}_n \qquad \text{for } n = 1, 2, 3, 4. \tag{17}$$

By invoking the spectral theorem, one obtains an expression for the diagonal correlations in configuration space $\mathbf{C}_n$ (independent of $\mathbf{k}$) by integrating over the correlations in momentum space $\mathbf{C}_n(\mathbf{k})$ corresponding to the Green functions $\mathbf{G}_n$ [7]:

$$\mathbf{C}_n = \int \mathbf{C}_n(\mathbf{k}) = \int \mathrm{d}\mathbf{k}\mathbf{R}\varepsilon\mathbf{L}\mathbf{A}_n, \qquad n = 1, 2, 3, 4, \tag{18}$$

where $\mathbf{R}$ and $\mathbf{L}$ are matrices constructed from the right and left eigenvectors of the eigenvalues of the *non-symmetric* matrix $\mathbf{\Gamma}$, and ε is a diagonal matrix with elements $\delta_{ij}/(\mathrm{e}^{\beta\omega_i} - 1)$ obtained from eigenvalues ω_i $(i = 1, \ldots, 12)$ in the case when all of them are not zero.

Unfortunately, equation (18) cannot be used directly because the 12×12 $\mathbf{\Gamma}$-matrix turns out to have four zero eigenvalues. These have to be treated properly when applying the spectral theorem in order to calculate the correlations. In [7] we have shown that in this case the correlations $\mathbf{C}_n(\mathbf{k})$ obey the equations

$$(1 - \mathbf{R}^0\mathbf{L}^0)\mathbf{C}_n(\mathbf{k}) = \mathbf{R}^1\varepsilon^1\mathbf{L}^1\mathbf{A}_n, \qquad n = 1, 2, 3, 4, \tag{19}$$

where

$$\mathbf{R} = (\mathbf{R}^0, \mathbf{R}^1), \qquad \mathbf{L} = \begin{pmatrix} \mathbf{L}^0 \\ \mathbf{L}^1 \end{pmatrix}. \tag{20}$$

The subscripts 0 and 1 label the matrices constructed from the right and left eigenvectors belonging to the zero and non-zero eigenvalues respectively, and ε^1 is a diagonal 8×8 matrix with elements $\delta_{ij}/(\mathrm{e}^{\beta\omega_i} - 1)$ obtained from the non-zero eigenvalues ω_i $(i = 1, \ldots, 8)$.

As written, equation (19) is formally correct but it still cannot be used directly for two reasons: (1) The matrix $(1 - \mathbf{R}^0\mathbf{L}^0)$ is a projection operator on the non-null space and thus has no inverse; i.e. we cannot isolate $\mathbf{C}_n(\mathbf{k})$ unless $(1 - \mathbf{R}^0\mathbf{L}^0)$ is independent of $\mathbf{k}$. In the example of [22], this is the case and one can take the projector outside the integral. This is not the case in the present example. (2) Even if $(1 - \mathbf{R}^0\mathbf{L}^0)$ were independent of $\mathbf{k}$, we still do not know how to treat the non-diagonal correlations $\mathbf{C}_{mn}$ of a multilayer problem.

We have considered these problems in recent publications [22, 23], where we show that a solution is attained via the singular value decomposition (see e.g. [24]) of the $\mathbf{\Gamma}$-matrix

$$\mathbf{\Gamma} = \mathbf{U}\mathbf{W}\tilde{\mathbf{V}} = \mathbf{u}\mathbf{w}\tilde{\mathbf{v}}, \tag{21}$$

where $\mathbf{U}$ and $\tilde{\mathbf{V}}$ are orthogonal matrices, and $\mathbf{W}$ is a diagonal matrix with the singular values on the diagonal, and $\mathbf{u}$ and $\tilde{\mathbf{v}}$ are matrices obtained from $\mathbf{U}$ and $\tilde{\mathbf{V}}$ by omitting the columns and rows corresponding to singular values zero. Multiplying equation (19) from the left by $\tilde{\mathbf{v}}$ and inserting $\mathbf{v}\tilde{\mathbf{v}} + \mathbf{v}_0\tilde{\mathbf{v}}_0 = 1$ gives

$$\tilde{\mathbf{v}}(1 - \mathbf{R}^0\mathbf{L}^0)\mathbf{C}_n(\mathbf{k}) = \mathbf{R}^1\varepsilon^1\mathbf{L}^1(\mathbf{v}\tilde{\mathbf{v}} + \mathbf{v}_0\tilde{\mathbf{v}}_0)\mathbf{A}_n, \tag{22}$$

and use of $\tilde{\mathbf{v}}\mathbf{R}^0 = 0$, $\mathbf{L}^1\mathbf{v}_0 = 0$, and $\mathbf{r} = \tilde{\mathbf{v}}\mathbf{R}^1$ and $\mathbf{l} = \mathbf{L}^1\mathbf{v}$ leads to the equations

$$\tilde{\mathbf{v}}\mathbf{C}_n(\mathbf{k}) = \mathbf{r}\varepsilon^1\mathbf{l}\tilde{\mathbf{v}}\mathbf{A}_n, \qquad n = 1, 2, 3, 4. \tag{23}$$

For more details of the formalism consult [23], where we present a systematic way of finding for each sublattice one $\mathbf{k}$-independent $\tilde{\mathbf{v}}$ vector having a layer structure, i.e. $\tilde{\mathbf{v}}_n = (0, \ldots, \tilde{v}_n, 0, \ldots, 0)$. In this way the non-diagonal correlations disappear from those rows in equation (23) corresponding to $\tilde{\mathbf{v}}_n$, and the $\mathbf{k}$-integration can be performed: $\int \mathrm{d}\mathbf{k}\, \tilde{\mathbf{v}}\mathbf{C}_n(\mathbf{k}) = \tilde{\mathbf{v}} \int \mathrm{d}\mathbf{k}\, \mathbf{C}_n(\mathbf{k}) = \tilde{\mathbf{v}}\mathbf{C}_n$. In the present case $\tilde{\mathbf{v}}_n$ is given by

$$\tilde{\mathbf{v}}_n = \left(\left(\frac{1}{\sqrt{2}}, -\frac{1}{\sqrt{2}}, 1\right)\delta_{1n}, \left(\frac{1}{\sqrt{2}}, -\frac{1}{\sqrt{2}}, 1\right)\delta_{2n}, \left(\frac{1}{\sqrt{2}}, -\frac{1}{\sqrt{2}}, 1\right)\delta_{3n}, \left(\frac{1}{\sqrt{2}}, -\frac{1}{\sqrt{2}}, 1\right)\delta_{4n}\right), \qquad n = 1, 2, 3, 4. \tag{24}$$

Putting equation (24) in (23) yields four equations which contain the eight magnetization components implicitly. The necessary additional four equations are obtained from the regularity conditions [7]

$$\int \mathrm{d}\mathbf{k}\, \mathbf{L}_0\mathbf{A}_n = \int \mathrm{d}\mathbf{k}\, \tilde{\mathbf{u}}_0\mathbf{A}_n = 0, \qquad n = 1, 2, 3, 4, \tag{25}$$

which are obtained from the fact that the commutator Green functions must be regular at the origin; see e.g. [25]. The $\tilde{\mathbf{u}}_0$ are constructed from the null-eigenvectors of the singular value decomposition of the matrix $\mathbf{\Gamma}$. The resulting eight integral equations are solved self-consistently by the curve-following method described in detail in the appendix of [26]. Note that the $\tilde{\mathbf{u}}_0$ are determined numerically only up to an orthogonal transformation. To ensure proper behaviour as a function of $\mathbf{k}$, $\tilde{\mathbf{u}}_0$ must be calibrated at each $\mathbf{k}$. A procedure for effecting this is presented in an appendix of [23].

3. Results

In the following we present results for the bilayer ferromagnet, the bilayer antiferromagnet, and the coupled ferro- and antiferromagnetic bilayer. All calculations are for an in-plane orientation of the spins of both layers. In each case we compare the results of Green function theory (GFT) with those of mean field theory (MFT) obtained by putting the momentum-dependent terms equal to zero.

In order to see the effects of the interlayer coupling most clearly, we use different exchange interaction strengths for both layers:

(a) FM–FM: $J_{1\mathrm{FM}} = 100$, $J_{2\mathrm{FM}} = 50$,
(b) AFM–AFM: $J_{1\mathrm{AFM}} = -100$, $J_{2\mathrm{AFM}} = -50$,
(c) FM–AFM: $J_{\mathrm{FM}} = 100$, $J_{\mathrm{AFM}} = -50$.

Because of the Mermin–Wagner theorem [27], one needs anisotropies in the Green function description: we assume $D^z = +1.0$ for FM layers and $D^x = -1.0$ for AFM layers. The magnitude of the anisotropies is appropriate for 3d transition metal systems. For a compensated interface, the magnetizations of the FM and AFM layers are almost orthogonal to each other even at $T = 0$ because of the interface exchange interaction J_{int}. We choose the FM magnetization to be oriented in the z-direction and the AFM magnetization in the x-direction. Our particular choice of the anisotropies supports this arrangement not only at $T = 0$ but also at finite temperatures. For other choices of anisotropies the magnetic arrangement could be different. The interlayer coupling is assumed to be positive for the ferromagnetic bilayer and negative for the antiferromagnetic bilayer. For the coupled FM–AFM system, both signs are used. We consider three interlayer coupling constants with strength $J_{\mathrm{int}} = 30$, 75, 160, respectively, one smaller than the weakest exchange interaction, one larger than the strongest exchange interaction, and one in between.

3.1. The ferromagnetic and the antiferromagnetic bilayers

Results for the FM and AFM bilayers are presented in this subsection. We do so in order to have a basis for discussing the differences to the coupled FM–AFM bilayer described later on.

In figure 1(a) we show the sublattice magnetizations of the ferromagnetic bilayer as a function of the temperature for three interlayer couplings calculated with Green function theory (GFT). The magnetization profiles are different for the two layers (the magnetization is larger for the layer with the larger exchange interaction) but end in a common Curie temperature, which increases with increasing strength of the interlayer coupling: $T_{\mathrm{Curie}} = 50.66$, 55.24, 60.04.

For the antiferromagnetic bilayer we use the same parameters as for the ferromagnetic bilayer except for a sign change. In figure 1(b) we show the sublattice magnetizations of the antiferromagnetic bilayer for two interlayer coupling strengths calculated with Green function theory. To make the figures more transparent we leave out the result for the intermediate interlayer coupling strength. The corresponding magnetization curves lie in between those of the other couplings. One observes clearly the well known reduction of the magnetizations at low temperatures due to quantum fluctuations, which are missing in MFT; see figure 1(c). Since $|J_{1\mathrm{AFM}}| > |J_{2\mathrm{AFM}}|$ this reduction is larger for the first layer. With increasing temperature the magnetization curves of the two layers cross each other, a fact which was first observed by Diep [11], and finally end in a common Néel temperature. A larger interlayer coupling leads to a larger suppression at low temperatures and to a larger Néel temperature. Whereas with the present choice of parameters the magnetization profiles of the FM and AFM bilayers are rather different at low temperatures, the critical temperatures turn out to be identical: $T_{\mathrm{Curie}} = T_{\mathrm{Néel}}$ (cf figures 1(a) and (b)), a fact that has already been discussed by Lines [28].

For comparison, we show in figure 1(c) the results of mean field theory (MFT) with the same parameters. The magnetization profiles as well as the critical temperatures are identical for the ferromagnetic and antiferromagnetic bilayers. As is well known, the Curie (Néel) temperatures ($T_{\mathrm{Curie\ (Néel)}} = 102.10$, 107.25, 123.16) are much larger in MFT due to the missing magnon excitations, with the present choice of parameters by about a factor of 2.

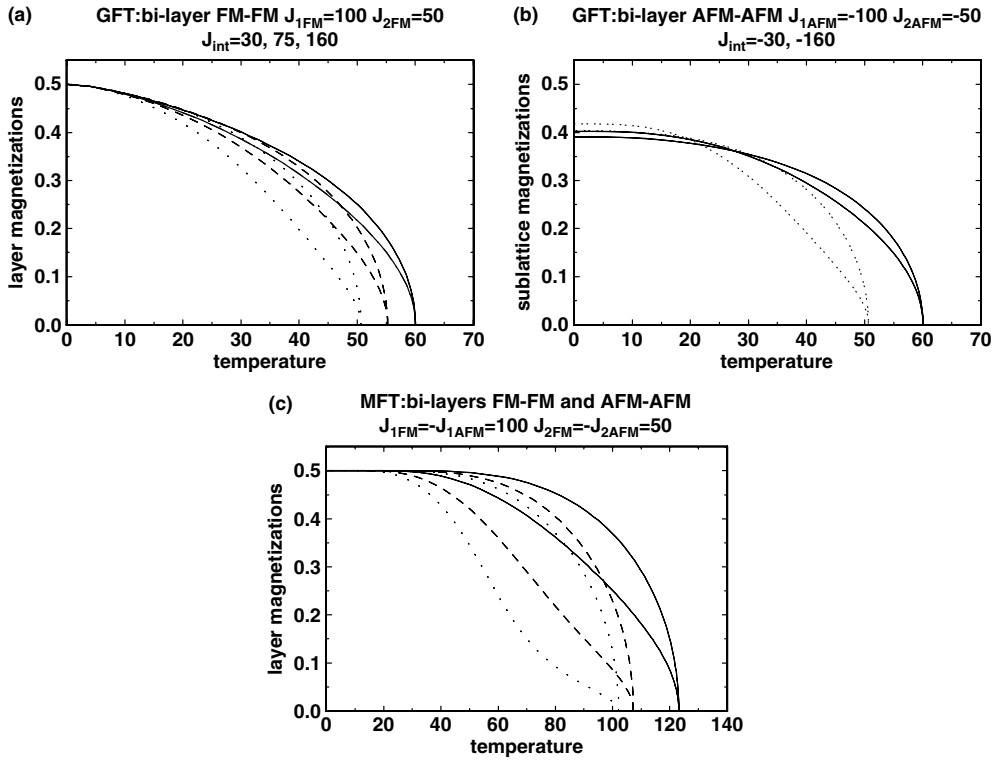

Figure 1. (a) Green function theory (GFT) for the ferromagnetic bilayer: the sublattice magnetizations are displayed as a function of the temperature for different interlayer couplings $J_{\rm int} = 30$ (dotted), 75 (dashed), 160 (solid). The exchange interaction and anisotropy constants are $J_{\rm 1FM} = 100$, $J_{\rm 2FM} = 50$, $D^z_{\rm 1FM} = 1.0$, $D^z_{\rm 2FM} = 1.0$. (b) GFT for the antiferromagnetic bilayer: the sublattice magnetizations are displayed as a function of the temperature for two interlayer couplings $J_{\rm int} = -30$ (dotted), -160 (solid). The exchange interaction and anisotropy constants are $J_{\rm 1AFM} = -100$, $J_{\rm 2AFM} = -50$, $D^x_{\rm 1AFM} = -1.0$, $D^x_{\rm 2AFM} = -1.0$. (c) Mean field theory (MFT) for the ferromagnetic and antiferromagnetic bilayers with identical parameters: $J_{\rm 1(2)FM} = |J_{\rm 1(2)AFM}|$, $D_{\rm 1(2)FM} = |D_{\rm 1(2)AFM}|$, $J_{\rm intFM} = |J_{\rm intAFM}|$.

Note that in MFT the Curie temperature is not very sensitive to the anisotropies, as long as they are much smaller than the exchange interaction. In GFT, however, the sensitivity is very much greater because of the Mermin–Wagner theorem [27] ($T_{\rm Curie(Néel)} \to 0$ for $D^{z(x)} \to 0$). One observes also that the effect of the interlayer coupling on the magnetization profiles is much stronger in MFT than in GFT.

3.2. The coupled ferro–antiferromagnetic bilayer

This is the most interesting case. In the present study, we consider two in-plane magnetization components of each sublattice, thus allowing non-collinear magnetizations in both the FM and AFM layers. Our computer code, when specialized to a single magnetization direction, reproduces the results of [13]. Without interlayer coupling, the code also reproduces the results for both the monolayer ferromagnet and monolayer antiferromagnet simultaneously. The present choice of anisotropies supports the orthogonal arrangement of the magnetizations of the FM and AFM layers favoured by the exchange interaction alone. The interlayer coupling

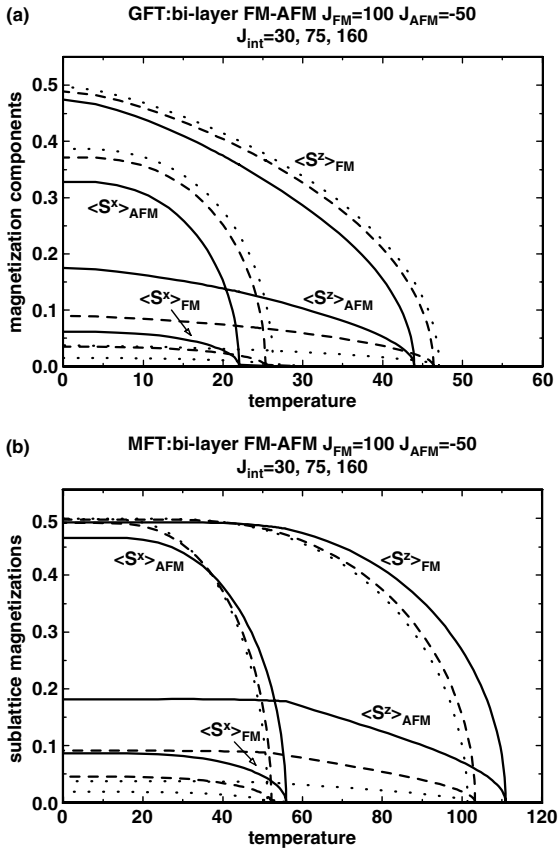

Figure 2. (a) Green function theory (GFT): the sublattice magnetizations of the ferro- and antiferromagnetic sublattices are displayed as a function of the temperature for different interlayer couplings $J_{\rm int} = 30, 75, 160$. The exchange interaction and anisotropy constants are $J_{\rm FM} = 100$, $J_{\rm AFM} = -50$, $D^x_{\rm AFM} = -1.0$, $D^z_{\rm FM} = 1.0$. (b) Mean field theory (MFT): with the same parameters.

destroys the perpendicular orientation of the ferromagnet (in the z-direction) with respect to the antiferromagnet (in the x-direction) even at temperature $T = 0$, as can be seen from figures 2 and 3. In figure 2(a) we show the sublattice magnetizations of an sc lattice calculated with GFT for three interlayer coupling strengths. With a positive interlayer coupling all sublattice magnetizations develop a positive z-component, whereas the x-components of the two sublattice magnetizations in each layer are oriented oppositely. With increasing temperature, all x-components decrease until they vanish at a common temperature $T^*_{\rm Néel}$, slightly above the Néel temperature of the uncoupled AFM. For $T > T^*_{\rm Néel}$ all sublattice magnetizations point in the positive z-direction, and the AFM layer assumes a ferromagnetic arrangement, and remains so until a common critical temperature $T_{\rm C}$ is reached, at which the magnetic order vanishes altogether. This is more clearly shown in figure 3 for the case of the strongest interlayer coupling of figure 2. Due to the strong interlayer coupling, the magnetizations of the layers are no longer collinear, even at $T = 0$, and they turn more and more into the z-direction with increasing temperature until $T^*_{\rm Néel}$, while the magnitudes of the magnetization vectors shrink. Above $T^*_{\rm Néel}$ the sublattice magnetizations stay collinear until they vanish at the critical temperature $T_{\rm C}$.

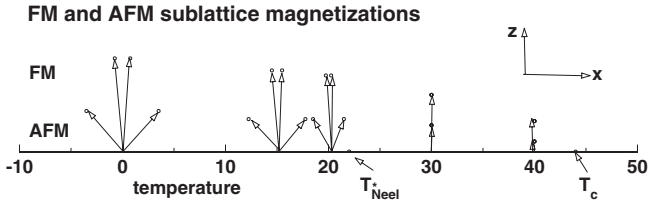

Figure 3. The reorientation of the sublattice magnetizations of the FM and AFM bilayer as a function of the temperature for the case of the strongest coupling ($J_{\rm int} = 160$) of figure 2.

With a negative interlayer coupling, the antiferromagnetic sublattice spins rotate with increasing temperature into the negative z-direction. For $T > T^*_{\rm Néel}$, the magnetizations of both layers point in opposite directions, i.e. one has a ferrimagnetic situation.

A remarkable behaviour can be seen in figure 2. With increasing interlayer coupling strength, the critical temperatures $T^*_{\rm Néel} = 26.24, 25.29, 22.00$ and $T_{\rm C} = 47.05, 46.34, 43.94$ decrease in GFT. This is in contrast to the behaviour in MFT ($T^*_{\rm Néel} = 51.19, 52.18, 55.86$, $T_{\rm C} = 101.37, 103.28, 110.94$), where the opposite is true (compare figures 2(a) and (b)). We attribute this surprising result to the quantum fluctuations taken into account in Green function theory but neglected in a mean field treatment. This behaviour depends, however, on the lattice type. It occurs for an sc lattice, whereas for fcc stacking an increase of $T_{\rm C}$ with increasing interlayer coupling is obtained as in MFT. We show this by deriving a formula for the critical temperature from GFT valid for both sc and fcc bilayers. The magnetizations are collinearly arranged as $T \to T_{\rm C}$, i.e. the x-components of the magnetizations vanish and the set of Green functions reduces to two decoupled (2×2) problems from which one can obtain via the spectral theorem two equations for the magnetizations of both layers. Denoting the ratio of the magnetizations by $\alpha_{\rm C} = \langle S^z_2 \rangle / \langle S^z_1 \rangle$ these equations become in this limit:

$$2T_{\rm C}\frac{1}{N}\sum_{\mathbf{k}}\frac{a_2}{a_1 a_2 - \alpha_{\rm C}(\gamma_{\rm int}(\mathbf{k})J_{\rm int})^2} = \frac{1}{2}, \tag{26}$$

$$2\alpha_{\rm C}T_{\rm C}\frac{1}{N}\sum_{\mathbf{k}}\frac{a_2}{a_1 a_2 - \alpha_{\rm C}(\gamma_{\rm int}(\mathbf{k})J_{\rm int})^2} = \frac{1}{2}, \tag{27}$$

with

$$\begin{aligned} a_1 &= q_0(J_1 + D^z_1) + \alpha_{\rm C} q_{\rm int} J_{\rm int} - \gamma_0(\mathbf{k})J_1, \\ a_2 &= \alpha_{\rm C} q_0(J_2 + D^z_2) + q_{\rm int} J_{\rm int} - \alpha_{\rm C}\gamma_0(\mathbf{k})J_2. \end{aligned} \tag{28}$$

For the notation see equations (8)–(12). The $\mathbf{k}$ summation is performed as an integral over the first Brillouin zone, and $T_{\rm C}$ is determined from a self-consistent solution of the integral equations (26), (27). Note that $T_{\rm C}$ is symmetric with respect to the sign of $J_{\rm int}$, if simultaneously $\alpha_{\rm C} \to -\alpha_{\rm C}$.

In figure 4 the results for the critical temperatures for sc and fcc stacking as a function of the interlayer coupling are shown. In the upper panel we see that for an sc lattice $T_{\rm C}$ decreases with increasing interaction strength in GFT, whereas it increases with increasing interlayer interaction strength in MFT. For fcc stacking, $T_{\rm C}$ increases with increasing interlayer interaction strength for both GFT and MFT. We attribute this behaviour to a different action of the quantum fluctuations in sc and fcc stacking. For large interlayer couplings the critical temperatures approach a saturation value in GFT, whereas they increase infinitely in MFT, which cannot be the correct behaviour.

We now investigate the results of a sign change of the interlayer coupling $J_{\rm int}$ for the case of an sc lattice. In figure 5 we display the sublattice magnetizations for the ferromagnetic–

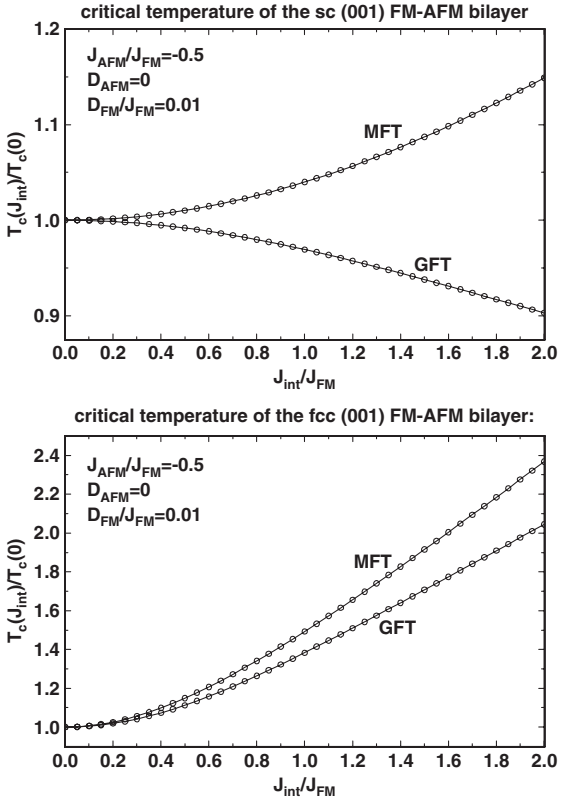

Figure 4. Critical temperatures $T_C(J_{int})$ as a function of the interlayer coupling J_{int} of an sc (upper panel) and a fcc (lower panel) FM–AFM bilayer (T_C is normalized to $T_C(J_{int} = 0)$). Results with mean field theory (MFT) and with Green function theory (GFT) are compared. Note the qualitatively different behaviour of the GFT results for sc and fcc stacking (see the text).

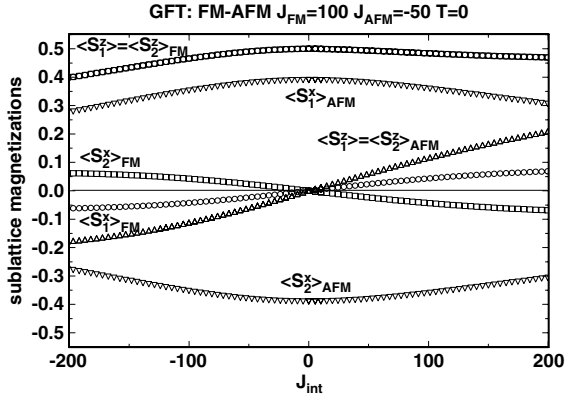

Figure 5. Sublattice magnetizations for the ferro–antiferromagnetic bilayer as a function of the interlayer coupling strength J_{int}.

antiferromagnetic bilayer at temperature $T = 0$ as functions of the interlayer coupling J_{int}. An asymmetric behaviour of the magnetizations is observed with respect to the sign of J_{int}.

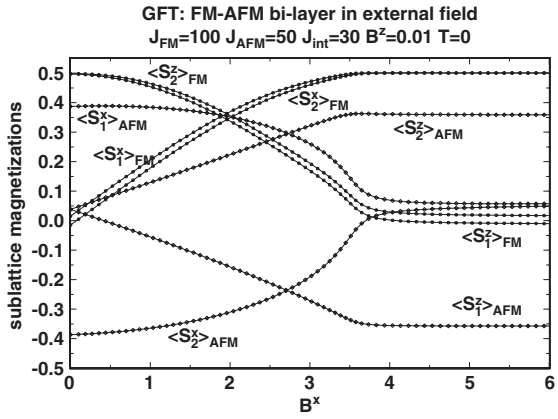

Figure 6. Sublattice magnetizations for the ferro–antiferromagnetic bilayer as a function of a field in the x-direction B^x and a small field B^z in the z-direction.

The z-components of the sublattice magnetizations are positive for positive interlayer couplings and negative for negative couplings, while the x-components of the magnetizations of the ferromagnetic sublattices interchange their roles. More interesting is that the magnitudes of the corresponding components of the sublattice magnetizations are not identical for $\pm J_{\rm int}$. This situation with respect to the sign of the interlayer coupling does not change at finite temperatures. We discuss this without showing a figure. When the x-components of the magnetizations vanish above the temperature $T^*_{\rm Néel}$, the magnetizations of the sublattices are collinear; for a positive interlayer coupling all z-components point in the positive z-direction, whereas for negative interlayer coupling the magnetizations of the antiferromagnetic sublattices point in the negative z-direction, i.e. opposite to the magnetizations of the ferromagnetic sublattices. The magnitudes of the magnetizations are larger for positive interlayer coupling. Even though the magnetization components are somewhat different for positive and negative interlayer couplings, numerical calculation and inspection of equations (26), (27) show that the corresponding critical temperatures are identical. We attribute the observed asymmetries in the magnetizations in GFT to quantum fluctuations in the non-collinear state, because there is no sensitivity on the sign of the interlayer coupling in MFT [6].

Finally, we discuss the influence of an external field on the sublattice magnetizations. As the only example we show in figure 6 the sublattice magnetizations at temperature $T = 0$ as a function of a field B^x in the direction of the AFM easy axis and a small perpendicular field component $B^z = 0.01$. At $B^x = 0$, one has a nearly orthogonal configuration of the FM (z-direction) and AFM (x-direction) layers. Owing to the positive interlayer coupling, both of the antiferromagnetic sublattice magnetizations have small positive z-components, and the ferromagnetic sublattice magnetizations have a small positive and a negative x-component. With increasing B^x, a field-induced magnetic reorientation occurs, i.e. both of the x-components of the magnetization of the ferromagnet become positive and increase, whereas the z-components decrease. For very large fields, the magnetization of the ferromagnet points almost in the x-direction. Accordingly, for a small B^x-field the AFM layer preserves its nearly antiferromagnetic configuration and the almost orthogonal magnetic arrangement with respect to the ferromagnetic layer. With increasing B^x, the AFM sublattice magnetizations rotate more and more into the z-direction, with two small positive x-components. The situation changes only slightly if one puts the z-component of the field to zero, $B^z = 0$. In this case the

main difference is that the reorientation transition is sharp at a reorientation field $B^x = 3.79$. The behaviour of the field dependence at finite temperatures is analogous, the only difference being that the magnetization components are reduced.

4. Concluding remarks

In the present paper we have developed a theory for coupling ferromagnetic and antiferromagnetic Heisenberg layers in the framework of many-body Green function theory. The new feature is that we allow a non-collinear orientation of the sublattice magnetizations for both of the ferromagnetic and antiferromagnetic layers. We applied the theory to bilayer systems with an in-plane orientation of the magnetizations. The theory yields results which are in many instances qualitatively similar to results previously obtained by mean field theory [6]. Owing to missing quantum fluctuations, MFT cannot, however, give the suppression of the magnetizations of the antiferromagnetic sublattices at low temperature. The main difference between MFT and GFT is, as for the uncoupled systems, the very different temperature scale.

An interesting effect is observed for the critical temperature T_C for systems with $J_{FM} > |J_{AFM}|$. For an sc lattice, T_C *decreases* with increasing interlayer coupling J_{int} in GFT, contrary to the behaviour in MFT, where the critical temperature *increases* with increasing J_{int}. For fcc stacking, however, for both GFT and MFT the critical temperature *increases* with increasing J_{int}. We attribute the different behaviour of the GFT results to a different action of the quantum fluctuations for sc and fcc stacking.

In the future we will study multilayer systems with mixed FM and AFM couplings. The code is written in such a way that it also allows the description of the coupling of ferromagnetic layers by an antiferromagnetic interlayer coupling and vice versa. Because we have already included magnetic fields, the theory may also be the basis for studying the exchange bias effect, where it seems, however, to be necessary to include interface disorder [21] in some way, for instance by introducing more sublattices per layer with different magnetic arrangements.

References

[1] Zuckermann M J 1973 *Solid State Commun.* **12** 745
Mata G J, Pestana E and Kiwi M 1982 *Phys. Rev.* B **26** 3841
Tersoff J and Falicov L M 1982 *Phys. Rev.* B **25** R2959
Tersoff J and Falicov L M 1982 *Phys. Rev.* **26** 459
Tersoff J and Falicov L M 1982 *Phys. Rev.* **26** 6186
Hasegawa H and Herman F 1988 *Phys. Rev.* B **38** 4863
Altbir D, Kiwi M, Martínez G and Zuckermann M J 1989 *Phys. Rev.* B **40** 6963
Mathon J, Villeret M, Muniz R B, d'Albuquerque e Castro J and Edwards D M 1995 *Phys. Rev. Lett.* **74** 3696
[2] For recent reviews see, e.g. Nogués J and Schuller I K 1999 *J. Magn. Magn. Mater.* **192** 203
Kiwi M 2001 *J. Magn. Magn. Mater.* **234/3** 584
Stamps R L 2000 *J. Phys. D: Appl. Phys.* **33** R247
[3] Néel L 1967 *Ann. Phys. Fr.* **2** 61
[4] Koon N C 1997 *Phys. Rev. Lett.* **78** 4865
[5] Hinchey L L and Mills D L 1986 *Phys. Rev.* B **33** 3329
Hinchey L L and Mills D L 1986 *Phys. Rev.* B **34** 1689
Cramer N and Camley R E 2001 *Phys. Rev.* **63** 060404(R)
Jensen P J and Dreyssé H 2002 *Phys. Rev.* **66** 220407(R)
[6] Jensen P J, Kiwi M and Dreyssé H 2005 *Eur. Phys. J.* B at press (*Preprint* cond-mat/0507265)
[7] Fröbrich P, Jensen P J, Kuntz P J and Ecker A 2000 *Eur. Phys. J.* B **18** 579
[8] Fröbrich P and Kuntz P J 2003 *Eur. Phys. J.* B **32** 445
[9] Wang H Y, Dai Z H, Fröbrich P, Jensen P J and Kuntz P J 2004 *Phys. Rev.* B **70** 134424
[10] Schwieger S, Kienert J and Nolting W 2005 *Phys. Rev.* B **71** 024428

[11] Diep H T 1991 *Phys. Rev.* B **40** 4818
Diep H T 1991 *Phys. Rev.* **43** 8509
[12] Wang H Y, Qian M and Wang E G 2004 *J. Appl. Phys.* **95** 7551
[13] Moschel A, Usadel K D and Hucht A 1993 *Phys. Rev.* B **47** 8676
[14] Moschel A and Usadel K D 1993 *Phys. Rev.* B **48** 13991
[15] Wang H Y and Dai Z H 2004 *Commun. Theor. Phys. (Beijing, China)* **42** 141
[16] Moschel A and Usadel K D 1994 *J. Magn. Magn. Mater.* **136** 99
[17] Qing'an L 2004 *Phys. Rev.* B **70** 014406
[18] Than Ngo V, Viet Nguyen H, Diep H T and Lien Nguyen V 2004 *Phys. Rev.* B **69** 134429
[19] Fröbrich P and Kuntz P J 2004 *Phys. Status Solidi* b **241** 925
[20] Fröbrich P and Kuntz P J 2004 *J. Phys.: Condens. Matter* **16** 3453
[21] Moran T J, Nogués J, Lederman D and Schuller I K 1998 *Appl. Phys. Lett.* **72** 617
Schulthess T C and Butler W H 1998 *Phys. Rev. Lett.* **81** 4516
Nowak U, Chantrell R W and Kennedy E C 2000 *Phys. Rev. Lett.* **84** 163
[22] Fröbrich P and Kuntz P J 2003 *Phys. Rev.* B **68** 014410
[23] Fröbrich P and Kuntz P J 2005 *J. Phys.: Condens. Matter* **17** 1167
[24] Press W H, Flannery B P, Teukolsky S A and Vetterling W T 1989 *Numerical Recipes* (Cambridge: Cambridge University Press)
[25] Nolting W 1986 *Quantentheorie des Magnetismus* vol 2 (Stuttgart: Teubner)
[26] Fröbrich P, Kuntz P J and Saber M 2002 *Ann. Phys., Lpz.* **11** 387
[27] Mermin N D and Wagner H 1966 *Phys. Rev. Lett.* **17** 1133
[28] Lines M E 1964 *Phys. Rev.* **133** A841